

# AN ASSESSMENT PROCEDURE INVOLVING WAVEFORM SHAPES FOR PUPIL LIGHT REFLEX

Minoru Nakayama

*CRADLE, Tokyo Institute of Technology, Tokyo 152-8552, Japan*

Wioletta Nowak

*Institute of Biomedical Engineering and Instrumentation, Wroclaw University of Technology, Wroclaw, Poland*

Hitoshi Ishikawa, Ken Asakawa

*School of Allied Health Sciences, Kitasato University, Sagami-hara 228-8555, Japan*

**Keywords:** Pupil light reflex, Waveforms, Fourier descriptor, Dissimilarity, Multidimensional scaling.

**Abstract:** The waveforms of Pupillary Light Reflex (PLR) can be analyzed in a diagnostic test that allows for differentiation between disorders affecting photoreceptors and those affecting retinal ganglion cells. This position paper proposes quantitative comparison metrics for waveform shapes using Discrete Fourier Transform (DFT) descriptors (FDs), and another procedure for emphasizing stimuli and subject differences using MultiDimensional Scaling (MDS) and clustering, where dissimilarities between stimuli are defined using descriptors as waveform features. To determine the efficiency of the procedures, a set of PLR data from a conventional experiment for the determination of a melanopsin-associated photoreceptive system was analyzed. Though the captured data was based on single trial for the stimuli, and the number of samples was small, both characteristics of stimuli and subjects were quantitatively extracted using the proposed procedures. Therefore, the possibility of applying the procedures to clinical diagnostics using PLR was examined.

## 1 INTRODUCTION

The Pupillary Light Reflex (PLR) is a well-known phenomenon, and recently its behavior has been examined in detail because of the existence of a melanopsin-associated photoreceptive system in the human retina, in addition to the conventional rod-cone system (Gamlin et al., 2007). Many studies have considered the contributions of this melanopsin to be a subset of intrinsically photosensitive retinal ganglion cells (Hattar et al., 2002; Dacey et al., 2005). To reveal the sensitivity and activity of these cells, the transient phase of PLR has often been studied using pupillary responses for low and high stimulus intensities, which were evoked using either short or long wavelength stimuli (Young and Kimura, 2008). In particular, the waveforms in the sustained phase of PLR are often compared across the stimulus conditions. These observations may be useful for clinical diagnostic procedures (Kawasaki and Kardon, 2007), though a quantitative index of PLR waveforms has not yet been established, however. In most cases,

waveform shapes are subjectively compared in pupillograms, therefore quantitative metrics and analytical procedures for corresponding waveforms have been desired. Because PLR observations are based on the response to a light pulse, human subjects cannot be subjected to repeated measurement. Also, a simplified procedure is required for clinical diagnostic tests. Though conventional pupil research has discussed mean pupil diameters and mean frequency spectra (Kuhlmann and Bottcher, 1999), these metrics cannot be applied. Simplified metrics of single waveforms are required to reveal the melanopsin-associated photoreceptive system.

In the area of signal processing and pattern recognition the features of waveforms using Fourier Descriptors have often been discussed (Zahn and Roskies, 1971; Pinkowski, 1994; Zhang and Lu, 2002). These waveforms can be compared to each other. Once the quantitative features are defined, the metrics of similarity or dissimilarity across the waveforms can also be extracted.

This position paper proposes a procedure for cre-

ating quantitative features of PLR waveforms, and demonstrates comparisons of these waveforms across stimuli and individuals using the metrics. Therefore, following topics are addressed:

1. A procedure for extracting feature vectors of PLR waveforms is created, and the metrics to compare these waveforms are determined.
2. The dissimilarities across the waveforms are also defined, and the differences in stimuli conditions and subjects are examined using multidimensional scoring and clustering techniques.

## 2 METHOD

### 2.1 Experimental Procedure

The Pupillary Light Reflex (PLR) is the constriction of the pupil elicited by an increase in illumination of the retina. A conventional experiment used for the determination of a melanopsin-associated photoreceptive system was conducted. In the experiment, a long wavelength (635nm bandwidth) red light and a short wavelength (470nm bandwidth) blue light were used at 2 different light intensities (10  $cd/m^2$  and 100  $cd/m^2$ ).

Both Figure ?? and 2 show the PLR of a 10 sec. light pulse as a constriction phase and a 10 sec. restoration phase in two normal subjects. In these figures, red lines show PLRs for long wavelengths, and blue lines show PLRs for short wavelengths. Also, solid lines show PLRs for high intensity light, and dotted lines show low intensity light. In this paper, the four conditions are defined as follows: r10 (long wavelength – low light intensity), r100 (long–high), b10 (short–low), b100 (short–high).

During this experiment, PLRs for these four conditions were observed for each subject.

Pupil light responses were recorded using an iris-tracker (Hamamatsu Iris-corder Dual). Subjects were 6 healthy individuals with normal vision between the ages of 20 and 21 years. Subjects were asked to not blink for 20 sec. while their pupil diameter was recorded at a sampling rate of 30 Hz. These measurements were taken in a dark room with constant lighting conditions. A dark-adaptation period of 5 minutes was allowed prior to taking all measurements.

### 2.2 Fourier Descriptors

The feature vectors for PLR waveforms were extracted using the Discrete Fourier Transform (DFT) procedure (Pinkowski, 1994; Zhang and Lu, 2002).

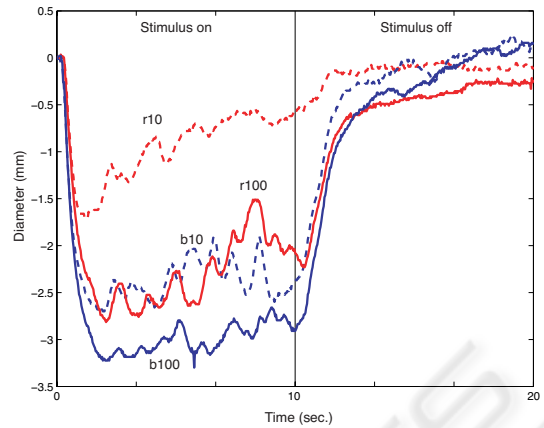


Figure 1: sub1.

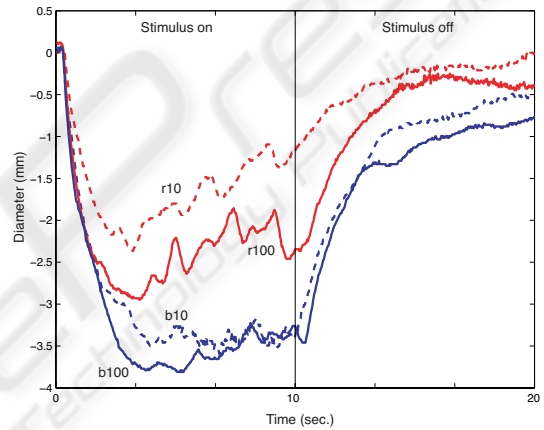


Figure 2: sub2.

As mentioned above, PLRs were sampled as discrete signals. Here, the length  $N$  of a discrete signal is defined as  $x(n)$ , which is sampled at time  $t$  with spacing  $\Delta$ . The signal  $x(n)$  can be noted as an equation (1) using DFT (Morishita and Kobatake, 1982).

$$x(n) = a_0 + \sum_{k=1}^{N/2} \left( a(k) \cos\left(2\pi k \frac{t(n)}{N\Delta}\right) + b(k) \sin\left(2\pi k \frac{t(n)}{N\Delta}\right) \right) \quad (1)$$

$$a_0 = X(1)/N$$

$$a(k) = 2 \operatorname{real}(X(k+1))/N$$

$$b(k) = 2 \operatorname{imag}(X(k+1))/N$$

This suggests that PLR waveforms can be represented using coefficients  $a_0$ ,  $a(k)$  and  $b(k)$  with periodical cosine and sine functions. To present the features of the waveform, the magnitude of coefficients is preferred, because coefficient  $b(k)$  is the imaginary part of a value. The magnitudes of coefficients,

including  $a_0$ ,  $FD_i (i = 0, \dots, N/2 - 1)$  are used as Fourier descriptors (FD) as follows in vector (2):

$$f = [FD_0, FD_1, \dots, FD_{N/2-1}] \quad (2)$$

In general, the components  $FD_0$ ,  $a_0$  in the equation (1), show the DC components of the signal. These DC components represent the amplitude, except the waveform shape consisting of frequency components. Also, features are affected by individual factors, so that a standardized feature is preferred as follows in vector (3) as follows (Zhang and Lu, 2002):

$$f = \left[ \frac{FD_2}{FD_1}, \frac{FD_3}{FD_1}, \dots, \frac{FD_{N/2-1}}{FD_1} \right] \quad (3)$$

Additionally, an appropriate number of components for the feature vector represent the characteristics of most signals only at the low-order values of 4 or 5 FDs (Pinkowski, 1994).

### 3 RESULTS

#### 3.1 Feature of PLRs

According to the analytical procedure in the above section 2.2, the features of PLRs for a subject (Sub1) were extracted. The actual calculations were conducted using MATLAB (Mathworks, Inc.). First,  $FD_0$  are extracted in order to compare the waveform amplitude as follows:

$$FD_{0,r10} = 319.4, FD_{0,r100} = 832.5, \\ FD_{0,b10} = 773.8, FD_{0,b100} = 1001.6$$

For  $FD_0$  values, the value for the b100 condition is the largest, and the value for r10 condition is the smallest. The order of these values coincides with the pattern in Figure ???. The  $FD_0$  values are extracted for all subjects and are illustrated in Figure 3. The order of these values is maintained across most subjects though individual differences are observed. In comparing PLRs between Sub1 and Sub2 in Figure ?? and 2, the relationships between the four conditions are different between the two subjects, though the orders of  $FD_0$  are almost similar to those in Figure 3.

Feature vectors are extracted for every waveform using the format of vector (3). For example, the set of vectors for a subject Sub1 is shown as follows:

$$f_{r10} = [0.408, 0.384, 0.197, 0.276, 0.150] \\ f_{r100} = [0.253, 0.289, 0.122, 0.204, 0.025] \\ f_{b10} = [0.177, 0.365, 0.071, 0.152, 0.072] \\ f_{b100} = [0.160, 0.289, 0.104, 0.141, 0.051]$$

According to the set of features, the vectors for b10 and b100 may be similar, but the vector for r10 is relatively different.

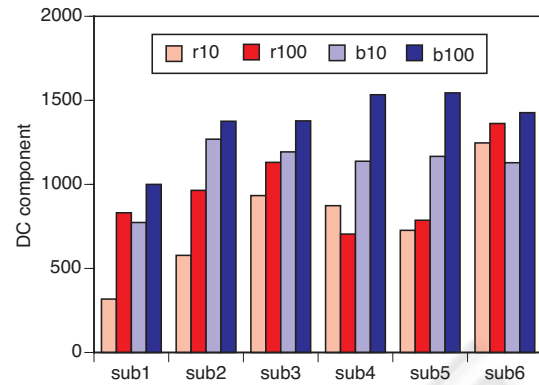


Figure 3: Comparison of DC components.

Table 1: Euclid distance between stimuli (sub1).

	r10	r100	b10	b100
r10	0			
r100	0.24	0		
b10	0.30	0.14	0	
b100	0.33	0.12	0.09	0

#### 3.2 Similarity/Dissimilarity

To compare the shape of waveforms quantitatively, metrics of similarity or dissimilarity should be defined using waveform feature vectors. This is a very popular approach for pattern recognitions such as categorization and discrimination (Stork et al., 2001). Here, the Euclidean distance (or Minkowski's power metric) can be defined as the Euclidean norm between two feature vectors. This is the dissimilarity metric. The distances amongst stimuli conditions for Sub1 are summarized in Table 1 as a triangular matrix. According to the matrix, the longest distance is between r10 and b100, and the shortest distance is between b10 and b100.

Distance matrices were created for all subjects.

#### 3.3 Configuration of Stimuli and Subjects

To create an overall structure of relationship between PLR waveforms, the Multi Dimensional Scaling (MDS) method is applied to the distance matrix. The famous application of MDS is re-creation of the geographical map of the distance matrix amongst cities (Takane, 2007). The Individual Difference MDS procedure has been introduced to extend the conventional MDS analysis to multiple distance matrices using every subject's matrix. The actual calculation was conducted using SAS (Mayekawa, 1997).

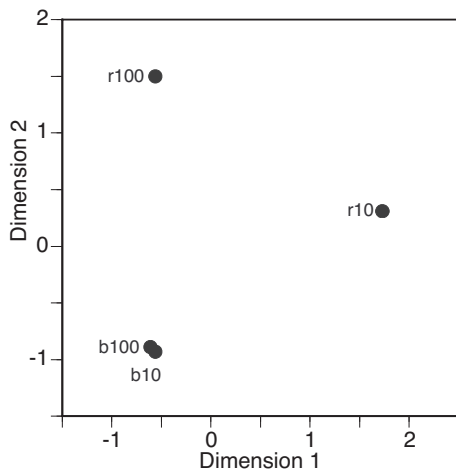


Figure 4: The stimulus configuration using two-dimensional scales from MDS.

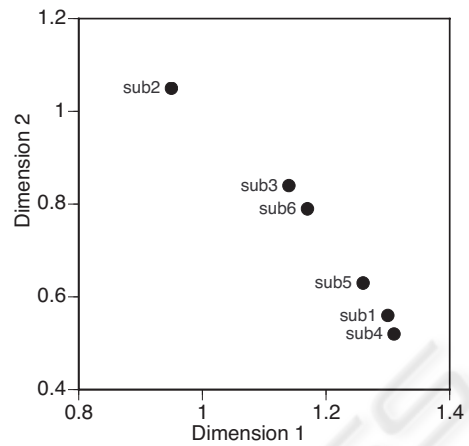


Figure 6: The subjects configuration using two-dimensional scales.

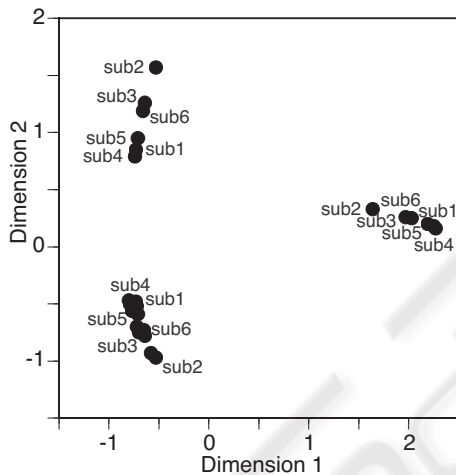


Figure 5: The stimulus for subjects configuration using two-dimensional scales.

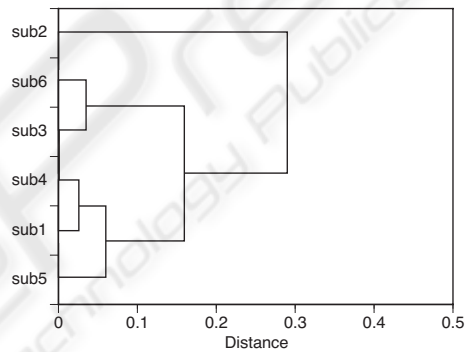


Figure 7: A dendrogram of the cluster for subjects.

First, the stimulus are configured on a two-dimensional space which is created by MDS analysis, as shown in Figure 4. The horizontal axis shows dimension 1, and the vertical axis shows dimension 2. Both dimensions are created as a result of MDS, therefore they show distance between stimuli while the dimensional interpretation is unstable. Both b10 and b100 almost overlap because the distance are the shortest. Both r10 and r100 are separated from b10 and b100, and the value of dimension 1 for r100 is almost the same as for b10 and b100. According to the two-dimensional configuration shown in Figure 4, the stimulus r10 differs from other conditions in both dimension 1 and dimension 2. In a sense, dimension 1 extracts r10 conditions while dimension 2 extracts r100 conditions.

All results for the four conditions and 6 subjects

are mapped in Figure 5. The stimuli conditions make clusters in response to the configurations of stimuli, as shown in Figure 4 where all subject's data is mapped in a similar style. When subjects' configuration inside three clusters are carefully observed, plots of subjects are shifted regularly in every cluster.

All subjects can be configured on the same space, as shown in Figure 6. Subjects are distributed on a line. Also, three clusters can be observed, configuration for one subject (Sub2) is separated from the others. To clarify the relationship between subjects, cluster analysis was conducted using two dimensional MDS information for each individual. A dendrogram is summarized in Figure 7. The horizontal axis shows averaged distance between subjects. The clustering process responds to the distribution of subjects in Figure 6. The distance between Sub1 and Sub4 is the shortest, and Sub2 is separated from the others.

The number of dimensions which are created by MDS analysis were extended to three dimension. The dimensional values are summarized in Table 2. The contribution of both dimension 1 and dimension 2 to

Table 2: Three dimensional information of MDS for stimuli.

	Dim1	Dim2	Dim3
r10	1.73	0.39	1.07
r100	-.60	1.46	-.12
b10	-.60	-1.03	0.62
b100	-.55	-.82	-1.57

the discrimination has the same tendency as in the case of a two-dimensional analysis. However, the stimuli b10 and b100 are separated from each other on a scale the same as in dimension 3, therefore dimension 3 may be related to the light strength of the short wavelength.

In this analysis, all subjects are normal individuals. This procedure can be used to detect diseases or as a diagnostic procedure if target patient data is separated from a cluster of normal subjects. This will be a subject of our further study.

#### 4 CONCLUSIONS

In this position paper, we propose a quantitative comparison metrics of Pupil Light Reflex (PLR) waveform shapes using the Discrete Fourier Transform (DFT) descriptors (FDs), and another procedure for emphasizing stimuli and subject differences using Multi Dimensional Scaling (MDS) and clustering when the dissimilarity between stimuli is defined using the descriptors as waveform features.

The demonstrations were conducted using a conventional experiment for the determination of a melanopsin-associated photoreceptive system. Though the captured data was based on single trial for the stimuli, and the number of samples was small, both characteristics of stimuli and subjects were quantitatively extracted using the proposed procedures. Therefore, the possibility of its application for clinical diagnostics using PLR was examined.

The interpretation of scales and clinical applications will be subjects of our further study.

#### REFERENCES

Dacey, D. M., Liao, H. W., and Peterson, B. B. (2005). Melanopsin-expressing ganglion cells in primate retina signal color and irradiance and project to the LGN. *Nature*, 433:749–754.

Gamlin, P. D., McDougal, D. H., and Pokorny, J. (2007). Human and macaque pupil responses driven by melanopsin-containing retinal ganglion cells. *Vision Research*, 47:946–954.

Hattar, S., Liao, H. W., and Takao, M. (2002). Melanopsin-containing retinal ganglion cells: architecture, projections, and intrinsic photosensitivity. *Science*, 295:1065–1070.

Kawasaki, A. and Kardon, R. H. (2007). Intrinsically photosensitive retinal ganglion cells. *Journal of Neuro-Ophthalmology*, 27:195–204.

Kuhlmann, J. and Böttcher, M., editors (1999). *Pupillography: Principles, Methods and Applications*. W. Zuckschwerdt Verlag, Munchen, Germany.

Mayekawa, S. (1997). *Multivariate Data Analysis Using SAS Software*. University of Tokyo Press, Tokyo, Japan.

Morishita, I. and Kobatake, H. (1982). *Signal Processing (In Japanese)*. The Society of Instrument and Control Engineers, Tokyo, Japan.

Pinkowski, B. (1994). Robust fourier descriptions for characterizing amplitude-modulated waveform shapes. *Journal of Acoustical Society of America*, 95(6):3419–3423.

Stork, D. G. R., Duda, O., and Hart, P. E. (2001). *Pattern Classification*. John Wiley & Sons, Inc., 2nd edition. Japanese translation by M. Onoue, New Technology Communications Co., Ltd., Tokyo, Japan (2001).

Takane, Y. (2007). Applications of multidimensional scaling in psychometrics. In Rao, C. and Sinharay, S., editors, *handbook of statistics 26 – Psychometrics*, pages 359–400. North-Holland, Amsterdam, Netherlands.

Young, R. and Kimura, E. (2008). Pupillary correlates of light-evoked melanopsin activity in humans. *Vision Research*, 48:862–871.

Zahn, C. T. and Roskies, R. Z. (1971). Fourier descriptors for plane closed curves. *IEEE Transaction on Computers*, Vol.C-21(3):269–281.

Zhang, D. and Lu, G. (2002). A comparative study on shape retrieval using fourier descriptors with different shape signatures. In *Proceedings of the 5th Asian Conference on Computer Vision*, pages 646–651. Springer.